# The role of the microenvironment in tumor invasion

Yangjin Kim* Sookkyung Lim†

**Abstract**

Fibroblasts and myofibroblasts in the tumor microenvironment are important players in tumor growth and metastasis because of their unique ability to coordinate events which increase cell proliferation and invasion especially in breast cancer. It has been experimentally shown that fibroblasts play an important role in promoting tumor growth. Our study illustrates a model in which tumor cells are able to communicate with these fibroblasts/myofibroblasts through proteinases for active invasion toward stroma near breast ducts.

## 1 Introduction

It is well established that tumor microenvironment affects tumor growth and metastasis [43]. Understanding the relationship between tumor and its microenvironment may lead to important new therapeutic approaches in controlling the growth and metastasis of cancer. Indeed, instead of targeting the tumor cells, one may target stromal elements in order to manipulate the host-tumor interaction in a way that it will confine the tumor [6, 31]. Thus, for instance, modulating cell adhesion or blocking Matrix Metalloproteinase (MMP) may be novel ways of confining cancer.

The tumor microenvironment includes various cell types such as epithelial cells, fibroblasts, myofibroblasts, endothelial cells and inflammatory cells. These cells communicate with one another and influence each other's behavior by means of the cytokines and growth factors they secrete. Fibroblasts are of particular interest because both *in vitro* and *in vivo* studies have shown that they contribute to the formation and growth of tumors [17]. A recent study of a chemotherapeutic drug for breast cancer, for instance, has found that a strong stroma reaction characterized by an increased number of fibroblasts surrounding the tumor is likely to have a bad response to this drug [12]. Myofibroblasts, described as activated fibroblasts with smooth muscle differentiation, are abundant in the stroma of malignant breast tissue, but rarely seen in normal breast tissue [44]. Active proliferation of myofibroblasts and, in turn, increased collagen deposition near tumor regions are characteristics of many solid tumors [48]. Whereas *in situ* carcinoma myofibroblasts predominantly reside in the immediate periphery of the developing carcinoma, after the transition to invasive breast cancer myofibroblasts migrate to the invading front [48, 15]. These differences in both the abundance and location of myofibroblasts most likely stem from signals sent by epithelial cells in which oncogenic changes have occurred.

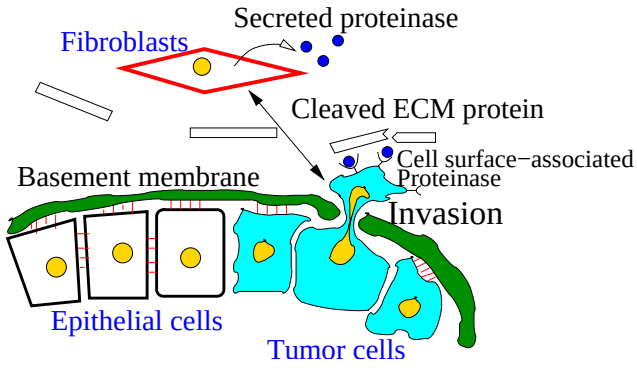


Figure 1: Illustration of tumor invasion *in vivo* [13, 21].

Initial expression of proteases in human breast cancer may be associated with the transition from Ductal Carcinoma *in Situ* (DCIS) to invasive ductal carcinoma. Expression studies of MMP in human DCIS material have shown that several classes of MMPs are expressed in periductal fibroblasts and myofibroblasts, indicating an intense stromal involvement during early invasion [2]. As reported in [14], disruption of the extracellular matrix (ECM) and cellular microenvironment caused by overexpression of MMPs-3,-7 or -14 in the mammary gland is sufficient to initiate mammary epithelial hyperplasia. See Figure 1.

In order to understand the interaction between tumor cells and fibroblasts/myofibroblasts at early stages of cancer, Kim *et al.* [22] considered an *in vitro* situation where transformed epithelial cells (TECs) and fibroblasts are placed in a transwell, separated by a semipermeable membrane (see also [16]). The results from experiments showed good agreement with the numerical results from the PDE model, and hence confirmed the

*Department of Mathematics & Statistics, University Michigan, Dearborn, MI 48128, USA

†Department of Mathematical Sciences, University of Cincinnati, Cincinnati, OH 45221, USA

model's ability to predict the behavior of tumor cells in response to signals from the stromal cells (fibroblasts). Other experiments were conducted with ECM-plated membrane to mimic a basement membrane. See [52, 21] for a review. These experiments measure the chemotactic force by which various molecules from one chamber attract tumor cells from another chamber. These experiments also quantify the influence of different compositions of the ECM layer on the invasion. Kim and Friedman also extended the previous model and monitored the entire invasion process *in silico*, in a setup which mimics experiments in a Boyden Invasion Assay, where a porous membrane coated by ECM is placed between two chambers [21, 22]. In their PDE model, both tumor cells and fibroblasts are allowed to migrate to other chambers. The model was used to explore several hypotheses on how to slow tumor growth and invasion.

In this paper we have developed a mathematical model of the early stage of cancer development when tumor epithelial cells in DCIS enter the vicinity of the basal membrane and may invade the stroma. The mathematical model is a mixture of mechanical equations and reaction-diffusion equations. The former describes the movement of the cells and the basal membrane in a viscous fluid and is solved by the immersed boundary (IB) method [38, 53, 29, 28]. The latter describes the concentrations of ECM and proteinases, and is solved by the alternating direction implicit (ADI) method together with the nonlinear system solver *nksol*. A new aspect of this paper is that we keep track of positions of tumor cells and stromal cells, and model breaches in the breast duct wall. Therefore, the mathematical model in this paper may provide a general framework that can be applicable in both industrial and theoretical settings, and it may also help researchers generate several hypotheses on how to block tumor invasion.

## 2 Mathematical model

In this section we first formulate equations of motion that describe how invasive TECs generate active forces and determine the direction of migration, and summarize an algorithm of the numerical method.

**2.1 Mechanics** In the model we consider tumor epithelial cells enclosed by the basal membrane. Both the basal membrane and the tumor cells can be represented by elastic closed loops immersed in a viscous fluid. Here the elastic membrane is tethered in stroma, see Figure 2. The IB method is used to simulate the interaction between the fluid and the structure (the tumor cells and the basal membrane). The fluid is governed by the incompressible Navier-Stokes equations.

Let $\boldsymbol{X}(s,t) = \boldsymbol{X}^c(s,t) \bigcup \boldsymbol{X}^B(s,t)$ be the configuration of the structure at any time $t$, where $s$ is a moving curvilinear coordinate. Here, $\boldsymbol{X}^c$ represents the cells which are surrounded by the basal membrane $\boldsymbol{X}^B$. The coupled system of equations of motion is as follows:

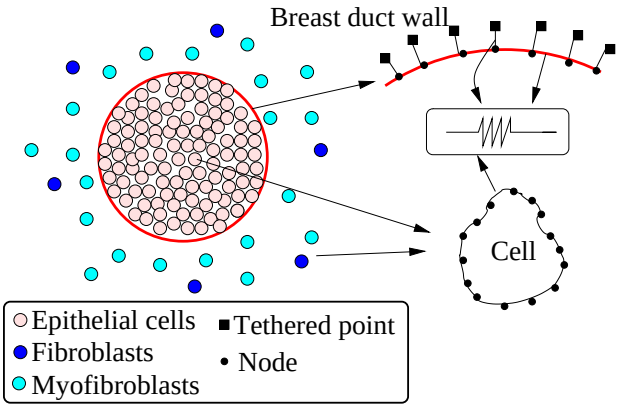


Figure 2: Illustration of our mechanics model.

$$\rho\left(\frac{\partial \boldsymbol{u}}{\partial t} + \boldsymbol{u}\cdot\nabla\boldsymbol{u}\right) = -\nabla p + \mu\Delta\boldsymbol{u} + \boldsymbol{f}, \tag{2.1}$$

$$\nabla\cdot\boldsymbol{u} = 0, \tag{2.2}$$

$$\boldsymbol{F} = \boldsymbol{F}^c_{\rm e} + \boldsymbol{F}^c_{\rm a} + \boldsymbol{F}^B_{\rm e} + \boldsymbol{F}^B_{\rm t}, \tag{2.3}$$

$$\boldsymbol{f}(\boldsymbol{x},t) = \int \boldsymbol{F}(s,t)\delta(\boldsymbol{x} - \boldsymbol{X}(s,t))ds, \tag{2.4}$$

$$\frac{\partial \boldsymbol{X}(s,t)}{\partial t} = \int \boldsymbol{u}(\boldsymbol{x},t)\ \delta(\boldsymbol{x} - \boldsymbol{X}(s,t))d\boldsymbol{x}. \tag{2.5}$$

Fluid Eqs. (2.1) and (2.2) are the Navier-Stokes equations of a viscous incompressible fluid. $\boldsymbol{u}(\boldsymbol{x},t)$ is the fluid velocity, $p(\boldsymbol{x},t)$ is the fluid pressure, and $\boldsymbol{f}(\boldsymbol{x},t)$ is the applied fluid force density defined on the fixed Cartesian coordinates $\boldsymbol{x} = (x_1, x_2)$. The constant parameters $\rho$ and $\mu$ in the fluid equations are the fluid density and the fluid viscosity, respectively.

Eq. (2.3) is the immersed boundary equation. $\boldsymbol{F}(s,t)$ is the force density which acts on the fluid by the immersed boundary. There are four contributions to the force density function $\boldsymbol{F}$: the elastic force density $\boldsymbol{F}^c_{\rm e}$ from the cell boundary, the active force density $\boldsymbol{F}^c_{\rm a}$ of cells for migration, the elastic force density $\boldsymbol{F}^B_{\rm e}$ from the membrane, and the tethered force density $\boldsymbol{F}^B_{\rm t}$ of the membrane. These force densities are given by

$$\boldsymbol{F}^c_{\rm e} = \frac{\partial E^c}{\partial \boldsymbol{X}^c}, \tag{2.6}$$

$$\boldsymbol{F}^B_{\rm e} = \frac{\partial E^B}{\partial \boldsymbol{X}^B}, \tag{2.7}$$

$$\boldsymbol{F}^B_{\rm t} = c_s(\mathbf{Z}^B - \boldsymbol{X}^B), \tag{2.8}$$

$$\boldsymbol{F}^c_{\rm a} = c_a \frac{P^n}{P^n + (k_P)^n}\vec{d}. \tag{2.9}$$

In Eqs. (2.6)-(2.7), $E^c$ and $E^B$ are the elastic energy functionals with respect to the configurations $\boldsymbol{X}^c$ and $\boldsymbol{X}^B$, respectively. In Eq. (2.8), $\mathbf{Z}^B$ is the reference configuration of the membrane and $c_s$ is the stiffness constant. In Eq. (2.9), $c_a$ is the force constant, $k_P$ is an invasiveness parameter, $n$ is the order in a Hill type function, and $\vec{d}$ is the unit vector in the moving direction, which depends on locations and concentrations of molecules in microenvironment. During invasion, the basal membrane is degraded by MMPs and this degraded portion will not generate the force as a result. We assume that there is a threshold of the basal body degradation to generate force and this threshold depends on the level of MMPs at the site.

Lastly, Eqs. (2.4)-(2.5) are the interaction equations that connect the fluid equations and the immersed boundary equation by the two-dimensional Dirac delta function $\delta$. Eq. (2.4) describes the relationship between the two corresponding force densities $\boldsymbol{f}(\boldsymbol{x},t)d\boldsymbol{x}$ and $\boldsymbol{F}(s,t)ds$. Eq. (2.5) is the no-slip condition, which means the structure moves at the local fluid velocity.

Let $\Omega = [0,1]\times[0,1]$ be the computational domain of the model in a two-dimensional space. To solve the above equations on $\Omega$ numerically, we discretized the equations in space and time using a finite difference scheme. In particular, we used FFTs (Fast Fourier Transform) to solve the discretized Navier-Stokes equations where the fluid domain is periodic. For a detailed description of the numerical scheme, the reader is referred to [37, 29].

**2.2 Reaction-diffusion** The governing equations for concentrations of ECM ($M$), tumor cell associated proteinase ($P$), and fibroblast-secreted proteinase ($G$) [21] are as follows:

$$\begin{aligned}\frac{\partial M}{\partial t} =& \underbrace{-a_1\ P\ \sum_i \frac{V_0}{V_*}\delta(\boldsymbol{x}-\boldsymbol{x}_i^n)}_{degradation}\\ &\underbrace{+a_2\sum_i \frac{V_0}{V_*}\delta(\boldsymbol{x}-\boldsymbol{x}_i^f)(1-M/M_*)}_{production},\end{aligned} \tag{2.10}$$

$$\begin{aligned}\frac{\partial P}{\partial t} =& \underbrace{\nabla\cdot(D_P\nabla P)}_{diffusion} + \underbrace{a_3\ \sum_i \frac{V_0}{V_*}\delta(\boldsymbol{x}-\boldsymbol{x}_i^n)}_{production}\\ &\underbrace{-a_4\ P}_{decay},\end{aligned} \tag{2.11}$$

$$\begin{aligned}\frac{\partial G}{\partial t} =& \underbrace{\nabla\cdot(D_G\nabla G)}_{diffusion} + \underbrace{a_5\ \sum_i \frac{V_0}{V_*}\delta(\boldsymbol{x}-\boldsymbol{x}_i^f)}_{production}\\ &\underbrace{-a_6\ G}_{decay},\end{aligned} \tag{2.12}$$

where $\boldsymbol{x}_i^n, \boldsymbol{x}_i^f$ are the sites of TECs and fibroblasts/myofibroblasts, respectively. $V_0$ and $V_*$ are the cell volume and reference ECM volume, respectively, and other parameters are positive constants. We prescribe Neumann boundary conditions:

$$D_P\nabla P\cdot\nu = 0 \ \text{ on } \partial\Omega,\ t>0, \tag{2.13}$$

$$D_G\nabla G\cdot\nu = 0 \ \text{ on } \partial\Omega,\ t>0, \tag{2.14}$$

where $\nu$ is the outward normal. We finally prescribe initial conditions:

$$\begin{aligned}&M(x,0) = M_0(x),\ P(x,0) = P_0(x),\\ &G(x,0) = G_0(x) \quad \text{in } \Omega.\end{aligned} \tag{2.15}$$

Equations (2.10)-(2.15) were solved on the same computational domain $\Omega$ using an ADI scheme [47] and a nonlinear solver *nksol* [5, 11] for algebraic systems. We solved these equations on a uniform grid with mesh width $h$=0.01 and used adaptive time stepping which adjusts the size of time step according to error and stability conditions. Since the center of motile tumor cells and source sites of migratory fibroblasts/myofibroblasts are not necessarily on the regular grid, these concentration values $(M,P,G)$ at the sites in the production/degradation terms were interpolated to grid points [24].

**2.3 An algorithm** We take the following algorithm for computation:

**step 0.** Initialization.

- **step 0.1** Set a regular, uniform grid for $\Omega$ and initialize concentrations of ECM ($M$), tumor-associated proteinase ($P$), and fibroblast-secreted proteinase ($G$) at each lattice point.
- **step 0.2** Set the locations of the basal membrane and fibroblasts outside the duct and tumor cells inside the duct.

**Step 1.** Locate all cells and basal membrane nodes that are within a given distance from cell $i$. Use the level of fibroblast-secreted proteinase in order to determine invasive cells and target the basal membrane to be degraded.

| | Description | Value |
|---|---|---|
| IB method | | |
| $l \times l$ | fluid domain | $0.5m \times 0.5m$ |
| $n \times n$ | grid size | $512 \times 512$ |
| $\mu$ | fluid viscosity | $100\ g/(cm \cdot s)$ |
| $\rho$ | fluid density | $1.35\ g/cm^3$ |
| $\triangle t$ | time step | $0.00125s$ |
| $r_c$ | radius of a tumor cell | $10\ \mu m$ |
| $r_{BM}$ | radius of a basal membrane | $103.5\ \mu m$ |
| $c_s$ | elastic stiffness of basal membrane | $2000\ g/(cm \cdot s^2)$ |
| $c_a$ | active force constant | $(3 \times 10^{-3} - 1.0 \times 10^{-2})\ dyne$ |
| $k_p$ | invasiveness parameter | $1.0 \times 10^{-10}\ g/cm^3$ |
| $G^{th}$ | a threshold for degradation of basal membrane | $3.2 \times 10^{-10}\ g/cm^3$ |
| Reaction-diffusion | | |
| $D_P^1$ | diffusion coefficient of tumor-associated proteinase (tissue) | $1.8 \times 10^{-12}\ cm^2/s$ |
| $D_P^2$ | diffusion coefficient of tumor-associated proteinase (duct) | $3.96 \times 10^{-12}\ cm^2/s$ |
| $D_G^1$ | diffusion coefficient of fibroblast-secreted proteinase (tissue) | $1.1 \times 10^{-7}\ cm^2/s$ |
| $D_G^2$ | diffusion coefficient of fibroblast-secreted proteinase (duct) | $1.11 \times 10^{-7}\ cm^2/s$ |
| $a_1$ | degradation of ECM by proteolytic activity of tumor cells | $1.29 \times 10^2\ s^{-1}$ |
| $a_2$ | release of ECM by fibroblasts/myofibroblasts | $3.43 \times 10^{-8}\ gcm^{-3}s^{-1}$ |
| $M_*$ | ECM carrying capacity | $5 \times 10^{-4} g/cm^3$ |
| $a_3$ | Production rate of tumor cell-associated proteinase | $1.5 \times 10^{-13}\ gcm^{-3}s^{-1}$ |
| $a_4$ | decay rate of tumor cell associated proteinase | $6.87 \times 10^{-5}\ s^{-1}$ |
| $a_5$ | fibroblast-secreted proteinase production rate | $5.74 \times 10^{-11}\ gcm^{-3}s^{-1}$ |
| $a_6$ | decay rate of fibroblast-secreted proteinase | $6.87 \times 10^{-5}\ s^{-1}$ |

Table 1: Computational parameters.

**Step 2.** Determine the moving direction of a cell when its invasion is activated. The migration direction is perpendicular to the tangent vector at the front node of invasive cells, i.e., cells cross the basal membrane by degradation.

**Step 3.** Deformation and translation of cells.

**Step 3.1** Find all the forces that act on the cell from each of the neighbor cells found in Step 1. Active forces are generated by invasive cells that has been activated by fibroblast-secreted proteinase at the site.

**Step 3.2** Determine whether proteinase levels reach the threshold value to degrade the basal membrane. When this happens, the degradation of the basal membrane occurs. This is done by removal of tethered forces from the basal membrane.

**Step 4.** Calculate the force density acting on the fluid by Eq. (2.3) and smear it out into the fluid grid by Eq. (2.4).

**Step 5.** Update the fluid velocity and fluid pressure using Eqs. (2.1)-(2.2).

**Step 6.** Move the structure at the new local fluid velocity using (2.5).

**Step 7.** Solve the reaction-diffusion equations (2.10)-(2.15) on a regular grid, using the ADI method, lagging the consumption term.

**Step 8.** Go to Step 1.

All parameter values used in this work are shown in Table 1 [41, 9, 23, 42, 21, 36, 33, 10, 50, 49, 4, 45, 23, 19]. The numerical scheme of the IB method is of first order accurate and the ADI method with *nksol* solver is of second order accurate.

## 3 Results

Figure 3 shows the typical time evolution of cell migration and a profile of the fibroblast-secreted proteinase at an early time when it initiates the basal membrane degradation and tumor cell invasion into the stroma. The sources of fibroblasts are located in the left center of the domain, $(x_i^f, y_i^f), i = 1, \ldots, 11$. The fibroblast-secreted proteinase at each site of fibroblasts diffuses to the vicinity of the breast duct which is located at the center of domain. Some TECs are activated to degrade the basal membrane in the neighborhood and begin to migrate toward the stroma, especially in the direction of fibroblasts for further tumor-stroma interaction.

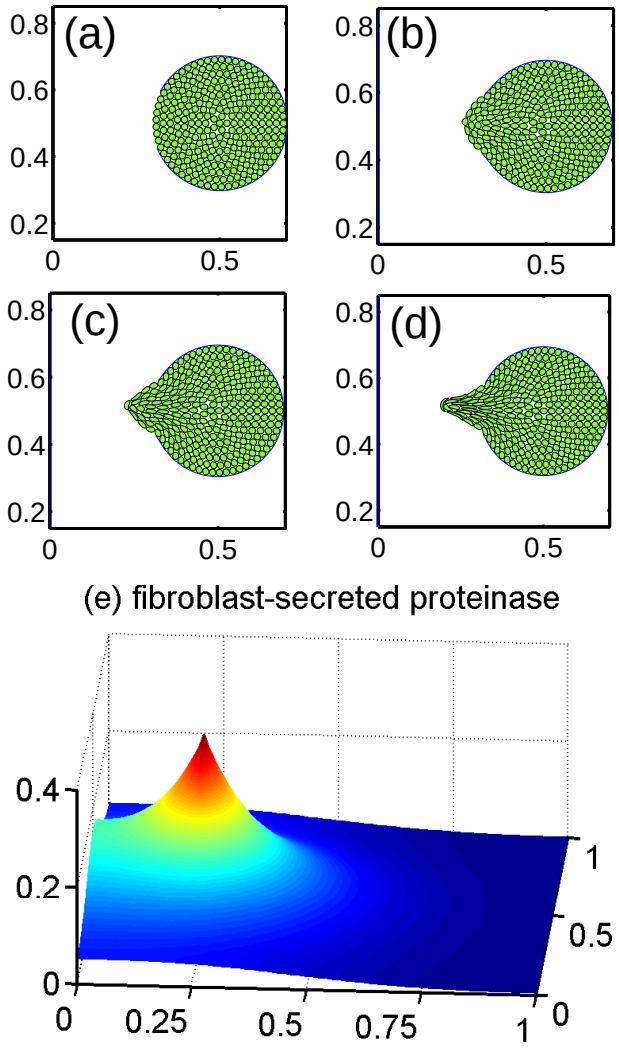


Figure 3: (a-d) Typical cell invasion at t=0 (a), t=20 (b), t=40, and (c) final time t=60 (d). (e) Profile of fibroblast-secreted proteinase at final time.

Figure 4 shows the time evolution of concentrations of ECM ($M$) and the tumor-associated proteinase ($P$) at the corresponding times, as shown in Figure 3. For illustration purposes, the domain of Figure 4(a-h) is $[0,0.5]\times[0,1]$ to show the migration region.

Note that the center of the breast duct was located at the center of the computational domain $\Omega$. As invading tumor cells migrate to the left, ECM is degraded by tumor-associated proteinase and continue to remodel the structure through reconstruction. This track of ECM and tumor-associated proteinase is associated with sites of migrating tumor cells. Fibroblast-secreted proteinase diffuses to the region near the duct, which initiates the degradation of the basal membrane by TECs inside the duct. Once this gate is open, TECs actively migrate into stroma. As TECs are activated to migrate into stroma, ECM is degraded by proteolytic activity via localized tumor-associated proteinase. A frontier cell, the first to escape, leads the way to further stromal regions by allowing space for cells inside a breast duct. Note that the deformation of the invasive cells occurs when they escape from the duct. This elongation of cells is experimentally observed when invasive cells are passing through the mechanically challenging structure, the basal membrane in the breast duct.

Figure 5 shows the effect of rate ($a_5$) of fibroblast-secreted proteinase production on invasiveness of tumor cells near a breast duct. Different dimensionless values of $a_5$ were used; $a_5$=20.0, 23.0, 24.0, 54.0, 94.0. As $a_5$ decreases, the initiation of basal membrane degradation slows down. Consequently, without whole or partial blocking of fibroblast-secreted proteinase, more cells enter into the stroma for further interaction with other cells such as immune cells and endothelial cells in a microenvironment leading to serious metastasis. Once tumor cells are out of the duct, it is much harder to control tumor growth due to their ability to obtain more genetic mutations through interaction with elements in the microenvironment and to modify the microenvironment [30, 7]. Due to the well-known role of MMPs, blocking the MMP pathway of tumor cells has been a common strategy by developing inhibitors of MMPs such as tissue inhibitor of metalloproteinases (TIMP), but has had little success. Instead of targeting the proteolytic activity of tumor cells within the duct, one can take a combined strategy of blocking both fibroblast-secreted proteinase and tumor-associated proteinase. Our results indicate that the early prevention of initiation of basal membrane degradation would be a much more effective way to block further tumor invasion into stroma.

Figure 6 illustrates the role of cell motility (fibroblasts) in the initiation of TEC invasion into the stroma. When these fibroblasts/myofibroblasts are not allowed

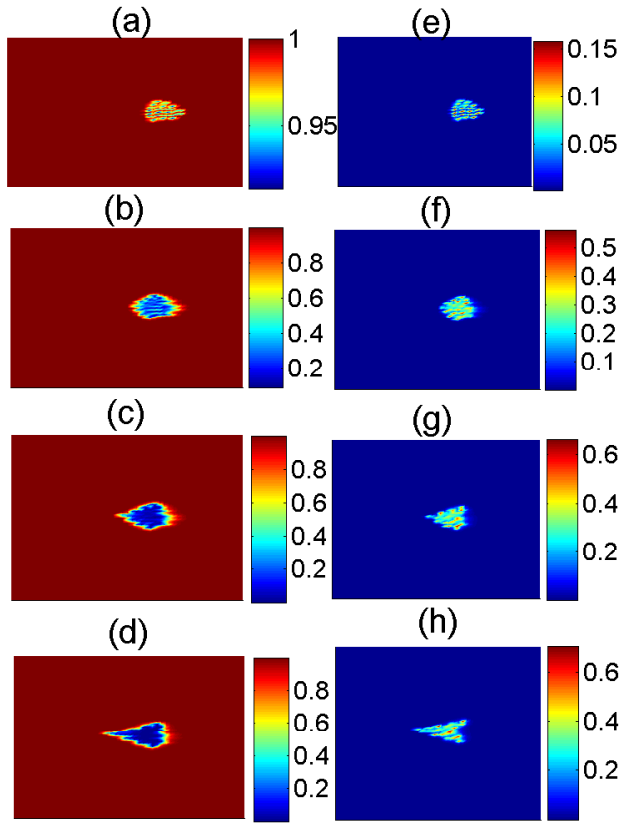


Figure 4: Time evolution of concentrations of ECM ($M$; (a-d)) and tumor-associated proteinase ($P$; (e-h)).

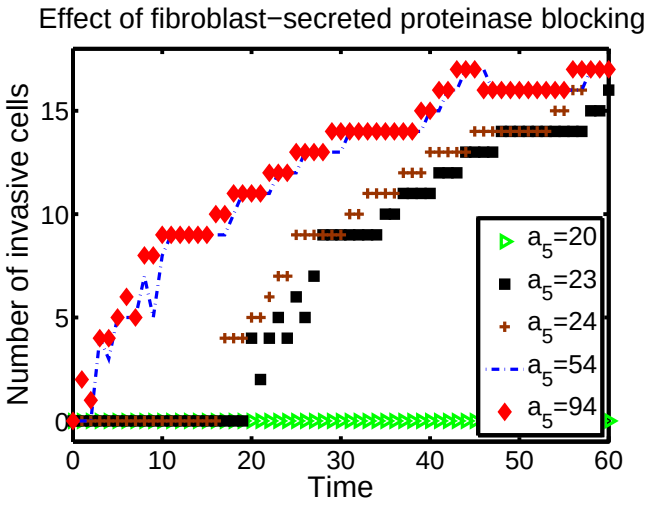


Figure 5: Effect of rate $a_5$ of fibroblast-secreted proteinase production on invasiveness of tumor cells.

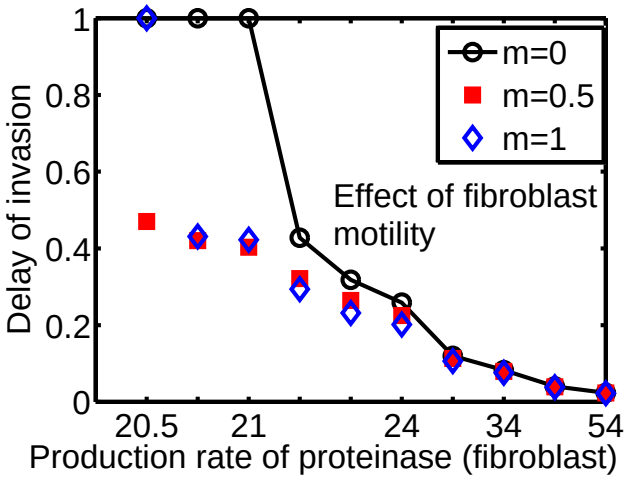


Figure 6: Role of fibroblast/myofibroblast motility in the initiation of tumor cell invasiveness.

to migrate toward the duct ($m = 0$), blocking the production of fibroblast-secreted proteinase ($G$) is effective, i.e., TEC does not initiate degradation of the basal membrane for the whole simulation time. However, when these fibroblasts/myofibroblasts are allowed to migrate toward the duct with a motility $m = 0.5$ or $m = 1$, the proteinase source from fibroblasts/myofibroblasts moves toward the duct to promote the initiation of basal membrane degradation by TECs within the duct. This result indicates that blocking of this proteinase is not enough to prevent the initiation of cancer invasion into the stromal region. A therapeutic drug that blocks both the fibroblast-secreted proteinase and fibroblast motility would be more effective at inhibiting the initiation of proteolytic activity of TECs within the duct.

## 4 Discussion and future work

This paper concerns the relationship between cancer and its microenvironment at the early stage of cancer development. More specifically, it considers invasive cancer. Understanding the relationship between a tumor and its microenvironment may lead to important new therapeutic approaches in controlling the growth and metastasis of cancer. Instead of targeting the tumor cells, one may target stromal cells in order to manipulate the host-tumor interaction in a way that prevents the tumor invasion. The changed (remodelled) microenvironment creates the elevated interstitial fluid pressure (IFP) creating chemoresistance. To improve the outcome of cancer therapy, researchers have developed several drugs targeting tumor associated fibroblasts (TAFs) or tumor associated macrophages (TAMs) [6]. The drugs targeting TAF include agents

for Platelet-derived growth factor receptor (PDGFR) (Imatinib [39], SU11248 [32], BAY43-9006 [51], CDP860 [18]) and fibroblast activation protein (Sibrotuzumab [25], DNA vaccine, PT-100 [1]). The goal of developing these drugs is to "normalize" IFP [6]. We note that FAP can function as a serine protease that cleaves ECM components such as gelatin and collagen, contributing to ECM remodeling [20].

Our numerical results indicate that the tumor invasion is reduced by introducing an inhibitor that blocks secretion of proteinase by fibroblasts/myofibroblasts. This means that we could target the FAP by developing more effective drugs using proven anti-FAP compounds such as Sibrotuzumab [25] and PT-100 [1]. However, our results also indicate that the fibroblasts may overcome the decrease in interaction with tumors due to the diffusion limit by active migration toward the duct in order to better promote tumor-stroma interaction. Therefore, one may need to inhibit the pathways of proteinase and motility-related proteins such as integrin, which is consistent with the current view of the importance of integrin as a therapeutic target in breast cancer metastasis [6]. Our simulation results show the non-uniform deformation of cells when they invade the stroma. This deformation of tumor cells is a typical but important process for migration through the basal membrane. It is not well understood how the basal membrane degradation and tumor invasion are coordinated, especially in the midst of chemical signals between stroma and tumor cells. Therefore, our model provides a general framework for understanding mechanical aspects of cell migration through the basal membrane as well as the role of various proteinases from both fibroblasts and tumor cells. The articles by Paszek *et al.* [34, 35] provide a review of the mechanical aspects of stroma-tumor interactions near a breast duct. In spite of tremendous efforts for anti-cancer drug development, the outcome is still poor and the microenvironment is blamed for this chemoresistance. Overall, our new model can be used to test the hypotheses on developing more effective chemo-agents systematically, connecting this academic theoretical framework to pharmaceutical industry.

The results of the present work can serve as a starting point for more comprehensive modeling and experimentation. The future model may include the following:
(a) Important molecules within the signalling pathways of the important communicators, epidermal growth factor (EGF) and Transforming growth factor (TGF-$\beta$); for example, anti-proliferation SMAD [26, 27, 8] and cytokines.
(b) Other important molecules in proteolytic activity such as plasminogen, Urokinase-type plasminogen activator (uPA) and TIMP [3].
(c) Mechanical feedback from the stroma near the breast duct known to be associated with tumor growth *in situ* as well as in modulation of progression/invasion in breast cancer [34, 35].
(d) Recruitment of inflammatory cells and angiogenesis which follows the lead of invasive TECs into the stroma, and contributes to an environment of metastatic potential [13].
Taking such factors into consideration will require multi-scale modeling that involves inter- and intracellular communication as well as cell population dynamics; some multiscale (hybrid) models have been developed in other contexts of tumor growth [24, 46].

While it is a good approximation of averaged cells, a partial differential equations model [21] is not capable of tracking the location and behavior of individual cells. To our knowledge, the IB method has not been applied to active cell migration in the context of breast cancer, although it has been used for cell proliferation [40]. While lattice-free, cell-based models for active cell migration [9] and passive tumor growth [21] have been suggested, the morphology of invasive cells has not been explored. Our model provides a novel approach to investigate the mechanical aspects of cell migration with better descriptions of cell structure. The current model also provides a framework for a multiscale model where intercellular processes (signal transduction pathways) can be taken into consideration. But any model that includes the intercellular processes will involve invasion at an early stage of cancer progression. In this sense the present paper is a first step toward more comprehensive models of invasion and metastasis.

## References


[1] S. Adams, G.T. Miller, M.I. Jesson, T. Watanabe, B. Jones, and B.P. Wallner. Pt-100, a small molecule dipeptidyl peptidase inhibitor, has potent antitumor effects and augments antibody-mediated cytotoxicity via a novel immune mechanism. *Cancer Res*, 64(15):5471–5480, 2004.

[2] K. Almholt, K.A. Green, A. Juncker-Jensen, B.S. Nielsen, L.R. Lund, and J. Romer. Extracellular proteolysis in transgenic mouse models of breast cancer. *J Mammary Gland Biol Neoplasia*, 12(1):83–97, 2007.

[3] C.B. Basbaum and Z. Werb. Focalized proteolysis: spatial and temporal regulation of extracellular matrix degradation at the cell surface. *Curr Opin Cell Biol*, 8(5):731–738, 1996.

[4] L.T. Bemis and P. Schedin. Reproductive state of rat mammary gland stroma modulates human breast cancer cell migration and invasion. *Cancer Res*, 60(13):3414–3418, 2000.

[5] P.N. Brown and Y. Saad. Hybrid krylov methods for

nonlinear systems of equations. *llnl report*, ucrl-97645, 1987.

[6] S.T. Chen, T.L. Pan, H.F. Juan, T.Y. Chen, Y.S. Lin, and C.M. Huang. Breast tumor microenvironment: proteomics highlights the treatments targeting secretome. *J Proteome Res*, 7(4):1379–1387, 2008.

[7] M.A. Chrenek, P. Wong, and V.M. Weaver. Tumour-stromal interactions. integrins and cell adhesions as modulators of mammary cell survival and transformation. *Breast Cancer Res*, 3(4):224–229, 2001.

[8] S.W. Chung, F.L. Miles, R.A. Sikes, C.R. Cooper, M.C. Farach-Carson, and B.A. Ogunnaike. Quantitative modeling and analysis of the transforming growth factor beta signaling pathway. *Biophys J*, 96(5):1733–1750, 2009.

[9] J. C. Dallon and H. G. Othmer. How cellular movement determines the collective force generated by the dictyostelium discoideum slug. *J. Theor. Biol.*, 231:203–222, 2004.

[10] P. Delvoye, P. Wiliquet, J.L. Leveque, B.V. Nusgens, and C.M. Lapiere. Measurement of mechanical forces generated by skin fibroblasts embedded in a three-dimensional collagen gel. *J Invest Dermatol*, 97(5):898–902, 1991.

[11] J.E. Dennis and R.B. Schnabel. *Numerical methods for unconstrained optimization and nonlinear equations*. Prentice-hall, 1983.

[12] P. Farmer, H. Bonnefoi, P. Anderle et al. A stroma-related gene signature predicts resistance to neoadjuvant chemotherapy in breast cancer. *Nat Med*, 15(1):68–74, 2009.

[13] D.H. Geho, R.W. Bandle, T. Clair, and L.A. Liotta. Physiological mechanisms of tumor-cell invasion and migration. *Physiology (Bethesda)*, 20:194–200, 2005.

[14] H.Y. Ha, H.B. Moon, M.S. Nam, J.W. Lee, Z.Y. Ryoo, T.H. Lee, K.K. Lee, B.J. So, H. Sato, M. Seiki, and D.Y. Yu. Overexpression of membrane-type matrix metalloproteinase-1 gene induces mammary gland abnormalities and adenocarcinoma in transgenic mice. *Cancer Res*, 61(3):984–990, 2001.

[15] N. Hanamura, T. Yoshida, E. Matsumoto, Y. Kawarada, and T. Sakakura. Expression of fibronectin and tenascin-c mrna by myofibroblasts, vascular cells and epithelial cells in human colon adenomas and carcinomas. *Int J Cancer*, 73(1):10–15, 1997.

[16] L.J. Hofland, .B. Burg, C.H. Eijck, D.M. Sprij, P.M. Koetsveld, and S.W. Lamberts. Role of tumor-derived fibroblasts in the growth of primary cultures of human breast-cancer cells: effects of epidermal growth factor and the somatostatin analogue octreotide. *Int J Cancer*, 60(1):93–99, 1995.

[17] A.V.D. Hooff. Stromal involvement in malignant growth. *Adv Cancer Res*, 50:159–196, 1988.

[18] G.C. Jayson, G.J. Parker, and S. Mullamitha et al. Blockade of platelet-derived growth factor receptor-beta by cdp860, a humanized, pegylated di-fab', leads to fluid accumulation and is associated with increased tumor vascularized. *J Clin Oncol*, 23(5):973–981, 2005.

[19] Y. Jia, Z.Z. Zeng, S.M. Markwart, K.F. Rockwood, K.M. Ignatoski, S.P. Ethier, and D.L. Livant. Integrin fibronectin receptors in matrix metalloproteinase-1-dependent invasion by breast cancer and mammary epithelial cells. *Cancer Res*, 64(23):8674–8681, 2004.

[20] T. Kelly. Fibroblast activation protein-alpha and dipeptidyl peptidase iv (cd26): cell-surface proteases that activate cell signaling and are potential targets for cancer therapy. *Drug Resist Updat*, 8(1-2):51–58, 2005.

[21] Y. Kim and A. Friedman. Interaction of tumor with its microenvironment : A mathematical model. *Bull. Math. Biol.*, in press [DOI 10.1007/s11538-009-9481-z], 2009.

[22] Y. Kim, A. Friedman, J. Wallace, F. Li, and M. Ostrowski. Transformed epithelial cells and fibroblasts/myofibroblasts interaction in breast tumor: A mathematical model and experiments. *J Math Biol,*, in press [DOI 10.1007/s00285-009-0307-2], 2009.

[23] Y. Kim, S. Lawler, M.O. Nowicki, E.A Chiocca, and A. Friedman. A mathematical model of brain tumor : pattern formation of glioma cells outside the tumor spheroid core. *J. Theo. Biol.*, 260:359–371, 2009.

[24] Y. Kim, M. Stolarska, and H.G. Othmer. A hybrid model for tumor spheroid growth in vitro i: Theoretical development and early results. *Math. Models Methods in Appl Scis*, 17:1773–1798, 2007.

[25] C. Kloft, E.U. Graefe, P. Tanswell, A.M. Scott, R. Hofheinz, A. Amelsberg, and M.O. Karlsson. Population pharmacokinetics of sibrotuzumab, a novel therapeutic monoclonal antibody, in cancer patients. *Invest New Drugs*, 22(1):39–52, 2004.

[26] M. Kretzschmar. Transforming growth factor-beta and breast cancer: Transforming growth factor-beta/smad signaling defects and cancer. *Breast Cancer Res*, 2(2):107-115, 2000.

[27] M. Kretzschmar, J. Doody, I. Timokhina, and J. Massague. A mechanism of repression of tgfbeta/ smad signaling by oncogenic ras. *Genes Dev*, 13(7):804–816, 1999.

[28] S. Lim and E. Jung. A three-dimensional model of a closed valveless pump system immersed in a viscous fluid. *SIAM Journal on Applied Mathematics*, to appear, 2010.

[29] S. Lim and C. S. Peskin. Simulations of the whirling instability by the immersed boundary method. *SIAM Journal on Scientific Computing*, 25(6):2066–2083, 2004.

[30] L.A. Liotta and E.C. Kohn. The microenvironment of the tumour-host interface. *Nature*, 411(6835):375–379, 2001.

[31] M. Loeffler, J.A. Kruger, A.G. Niethammer, and R.A. Reisfeld. Targeting tumor-associated fibroblasts improves cancer chemotherapy by increasing intratumoral drug uptake. *J Clin Invest*, 116(7):1955–1962, 2006.

[32] D.B. Mendel, A.D. Laird, and X. Xin et al. In vivo antitumor activity of su11248, a novel tyrosine kinase

inhibitor targeting vascular endothelial growth factor and platelet-derived growth factor receptors:. *Clin Cancer Res*, 9(1):327–337, 2003.

[33] P. Namy, J. Ohayon, and P. Tracqui. Critical conditions for pattern formation and in vitro tubulogenesis driven by cellular traction fields. *J Theor Biol*, 227(1):103–120, 2004.

[34] M. J. Paszek and V. M. Weaver. The tension mounts: mechanics meets morphogenesis and malignancy. *J Mammary Gland Biol Neoplasia*, 9(4):325–342, 2004.

[35] M. J. Paszek, N. Zahir, K. R. Johnson, J. N. Lakins, G. I. Rozenberg, A. Gefen, C. A. Reinhart-King, S. S. Margulies, M. Dembo, D. Boettiger, D. A. Hammer, and V. M. Weaver. Tensional homeostasis and the malignant phenotype. *Cancer cell*, 8(3):241–254, 2005.

[36] A.J. Perumpanani and H.M. Byrne. Extracellular matrix concentration exerts selection pressure on invasive cells. *Eur J Cancer*, 35(8):1274–1280, 1999.

[37] C. S. Peskin and D. M. McQueen. Fluid dynamics of the heart and its valves. *Case Studies in Mathematical Modeling: Ecology, Physiology, and Cell Biology*, H. G. Othmer, F. R. Adler, M. A. Lewis, and J. C. Dallon, eds., Prentice–Hall, Englewood Cliffs, NJ, 309–337, 1996.

[38] C. S. Peskin. The immersed boundary method. *Acta Numerica*, 11:479–517, 2002.

[39] K. Pietras, K. Rubin, T. Sjblom, E. Buchdunger, M. Sjquist, C.H. Heldin, and A. Ostman. Inhibition of pdgf receptor signaling in tumor stroma enhances antitumor effect of chemotherapy. *Cancer Res*, 62(19):5476–5484, 2002.

[40] K.A. Rejniak. A single-cell approach in modeling the dynamics of tumor microregions. *Mathematical Biosciences and Engineering*, 2(3):643–655, 2005.

[41] K.A. Rejniak and R.H. Dillon. A single cell-based model of the ductal tumour microarchitecture. *Computational and Mathematical Methods in Medicine*, 8(1):51–69, 2007.

[42] S. Saffarian, I.E. Collier, B.L. Marmer, E.L. Elson, and G. Goldberg. Interstitial collagenase is a brownian ratchet driven by proteolysis of collagen. *Science*, 306(5693):108–111, 2004.

[43] M. Samoszuk, J. Tan, and G. Chorn. Clonogenic growth of human breast cancer cells co-cultured in direct contact with serum-activated fibroblasts. *Breast Cancer Res*, 7:R274–R283, 2005.

[44] A.P. Sappino, O. Skalli, B. Jackson, W. Schurch, and G. Gabbiani. Smooth muscle differentiation in stromal cells of malignant and non-malignant breast tissue. *Int. J. Cancer*, 41:707–712, 1988.

[45] T. Shiomi and Y. Okada. Mt1-mmp and mmp-7 in invasion and metastasis of human cancers. *Cancer Metastasis Rev*, 22(2-3):145–152, 2003.

[46] M. Stolarska, Y. Kim, and H.G. Othmer. Multiscale models of cell and tissue dynamics. *Phil. Trans. Roy. Soc. A*, 367:3525–3553, 2009.

[47] J. C. Strikwerda. *Finite Difference Schemes and Partial Differential Equations*. Chapman & Hall, 1989.

[48] T.D. Tlsty. Stromal cells can contribute oncogenic signals. *Semin Cancer Biol*, 11(2):97–104, 2001.

[49] B. Vailhe, X. Ronot, P. Tracqui, Y. Usson, and L. Tranqui. In vitro angiogenesis is modulated by the mechanical properties of fibrin gels and is related to alpha v beta3 integrin localization. *In Vitro Cell. Dev. Biol.-Animal*, 33:763–773, 1997.

[50] R. B. Vernon, J. C. Angello, M. L. Iruela-Arispe et al. Reorganization of basement membrane matrices by cellular traction promotes the formation of cellular networks in vitro. *Lab. Invest.*, 66:536–547, 1992.

[51] S.M. Wilhelm, C. Carter, L. Tang et al. Bay 43-9006 exhibits broad spectrum oral antitumor activity and targets the raf/mek/erk pathway and receptor tyrosine kinases involved in tumor progression and angiogenesis. *Cancer Res*, 64(19):7099–7109, 2004.

[52] K. Yuan, R.K. Singh, G. Rezonzew, and G.P. Siegal. *Cell Motility in Cancer Invasion and Metastasis*, volume 8 of *Cancer Metastasis - Biology and Treatment*, chapter In Vitro Matrices for Studying Tumor Cell Invasion, 25–54. Springer, Netherlands, July 2006. ECM.

[53] L. Zhu and C. S. Peskin. Simulation of a flapping flexible filament in a flowing soap film by the immersed boundary method. *Journal of Computational Physics*, 179:452–468, 2002.